Fundamentals of Synthesis, Sintering Issues, and Chemical Stability of $BaZr_{0.1}Ce_{0.7}Y_{0.1}Yb_{0.1}O_{3-\delta}$ Proton Conducting Electrolyte for SOFCs

Armin VahidMohammadi* **and Zhe Cheng****,z**

Department of Mechanical and Materials Engineering, Florida International University, Miami, Florida 33174, USA

Fundamentals of synthesis, sintering issues, and chemical stability of $BaZr_{0.1}Ce_{0.7}Y_{0.1}Yb_{0.1}O_{3-\delta}$ (BZCYYb) proton conducting electrolyte material were studied. Solid state reaction (SSR) and glycine nitrate process (GNP) methods were used to synthesize BZCYYb powders. The GNP method produced powders with higher purity and smaller particle size in reduced heat-treatment time and temperature. It was found that BZCYYb material, despite its high proton conductivity, has surprisingly high tendency to react with common substrate materials including alumina, zirconia, and even ceria during high temperature sintering. This led to significant barium loss and even disintegration of the perovskite phase. In addition, during sintering, BZCYYb also lost Ba through gas phase. The barium loss and unwanted side reactions with substrates could be suppressed either using enclosure of a platinum substrate and a cover or protective layers of BZCYYb powders. On the other hand, using metal oxide sintering aids such as NiO helps reducing sintering time and temperature which mitigates the extent of unwanted reactions. Finally, isothermal exposure experiments showed that at 750°C, chemical stability limits for BZCYYb in CO_2 and H_2S contaminated atmospheres are below ~50 vol. % of CO_2 and between 50 and 100 ppm of H_2S, respectively, and they shift to lower values for Ba-deficient BZCYYb.
 [DOI: 10.1149/2.0021508jes]

Manuscript submitted April 2, 2015; revised manuscript received April 21, 2015. Published May 2, 2015.

There has been growing interest in proton conducting solid oxide fuel cells. In this type of solid oxide fuel cells (SOFCs), the electrolyte layer is usually a proton conducting oxide with ABO_3 perovskite structure.[1–3] When compared with oxygen ion conducting SOFCs, proton conducting SOFCs due to low activation energy required for proton conduction, can operate at lower temperatures (300–750°C),[1,3,4] which lowers operational costs and need for high temperature materials technology. Barium cerate and zirconate based oxides such as $BaCe_{1-x}Y_xO_{3-\delta}$ and $BaZr_{1-x}Y_xO_{3-\delta}$ are considered as the most practical proton conducting oxides used in intermediate temperature SOFCs (IT-SOFCs).[1–3,5,6] It is worth mentioning most of the currently used proton conducting materials are electron (hole) conductive at certain temperature ranges and therefore, these materials are also known as mixed ion and electron conductors (MIECs).[6]

Recently, $BaZr_{0.1}Ce_{0.7}Y_{0.1}Yb_{0.1}O_{3-\delta}$ (BZCYYb) has received huge interest as a promising proton conducting electrolyte material for SOFCs.[4,6–16] BZCYYb, which is a barium zirconate-cerate based oxide that is co-doped with Y and Yb, was first reported by Yang et al.[7] as a promising electrolyte material with very high proton conductivity. This material has ionic conductivity of ~0.06 Scm^{-1} at 700°C in humidified O_2 atmosphere, and it is reported to show higher ionic conductivity values at temperatures below 750°C compared with other common SOFC electrolyte materials such as $Gd_{0.1}Ce_{0.9}O_2$ (GDC) or $BaZr_{0.1}Ce_{0.7}Y_{0.2}O_{3-\delta}$ (BZCY).[7–12] Anode supported cells based on Ni-BZCYYb anode and BZCYYb electrolyte have been reported to produce power density of ~1.1 W/cm^2 and ~0.66 W/cm^2 at 750°C and 650°C, respectively.[7] In addition, BZCYYb-based SOFCs have been shown to have significantly better tolerance to coking and H_2S poisoning.[7,8] For example, it has been reported that power output of an anode-supported cell with thin electrolyte layer of BZCYYb did not change when the fuel was switched from pure hydrogen to ones contaminated with up to 30 ppm H_2S, indicating good chemical stability and excellent electrochemical activity of this material.[7]

Even though BZCYYb has been shown to have improved ionic conductivity compared to other barium-cerate or barium-zirconate based proton conducting electrolytes,[6–12] there are concerns with sintering and thermo-chemical stability of this material since similar issues have been previously reported for barium-cerate materials containing low contents of Zr.[13,14] BZCYYb usually needs very high sintering temperatures (>1500°C) for relatively long times (at least 10 h)[7–12] to be sintered to densities above 90% of theoretical density (TD). However, some Ba loss and structural disintegration have been previously reported for barium cerate based oxides under these high temperature sintering conditions.[13,14] This results in loss of perovskite structure and low density of sintered samples.[13,14] Different approaches have been investigated to overcome sintering issues of BZCYYb material and lower the sintering temperature which include two-step sintering,[15] adjusting BZCYYb powder properties by using different synthesis method other than conventional solid state reaction (SSR) method,[16] or using 1 wt.% NiO as a sintering aid.[8] On the other hand, current data in literature[7,8,15–17] have not provided understandings for observed variation in BZCYYb sintering issues and there is still a lack of fundamental study on chemical interactions during sintering process of this material.

In terms of chemical stability, there are very few reports in the literature on BZCYYb, especially the upper stability limit of this material. Yang et al.[7] reported that BZCYYb is chemically stable in atmospheres containing 50 vol. % CO_2 or 50 vol. % H_2O at 750°C for 300 h. In their report, it was also shown that this material is chemically stable in 50 ppm H_2S balanced by H_2 atmosphere at 750°C for 50 h. Addition of BZCYYb to conventional Ni-YSZ anode is also reported to significantly improve the sulfur tolerance of the anode.[18] However, these reports are in contradiction with poor chemical stability previously reported for $BaCe_{0.9-x}Zr_xY_{0.1}O_{3-\delta}$ with low contents of Zr dopant (<0.3) under CO_2 and H_2S contaminated atmospheres.[1–3,13,14] Therefore, lack of sufficient data in literature for chemical stability of BZCYYb material under different contaminated atmospheres brings the need for further studies on behavior of this material when exposed to contamination.

In this paper, we report new findings on synthesis, sintering issues, and chemical stability of BZCYYb as an electrolyte material for proton conducting SOFCs. The material was synthesized using both conventional SSR and glycine nitrate process (GNP) methods. A comprehensive study on different issues and parameters effecting sintering of BZCYYb has been carried out. Effects of powder synthesis route, sintering time and temperature, addition of sintering aids, different substrate types, and other sintering conditions have been studied to understand major factors contributing to obtaining high density BZCYYb disks while maintaining perovskite structure. Meanwhile, chemical stability of both BZCYYb disks and powders (stoichiometry

*Electrochemical Society Student Member.
**Electrochemical Society Active Member.
zE-mail: zhcheng@fiu.edu

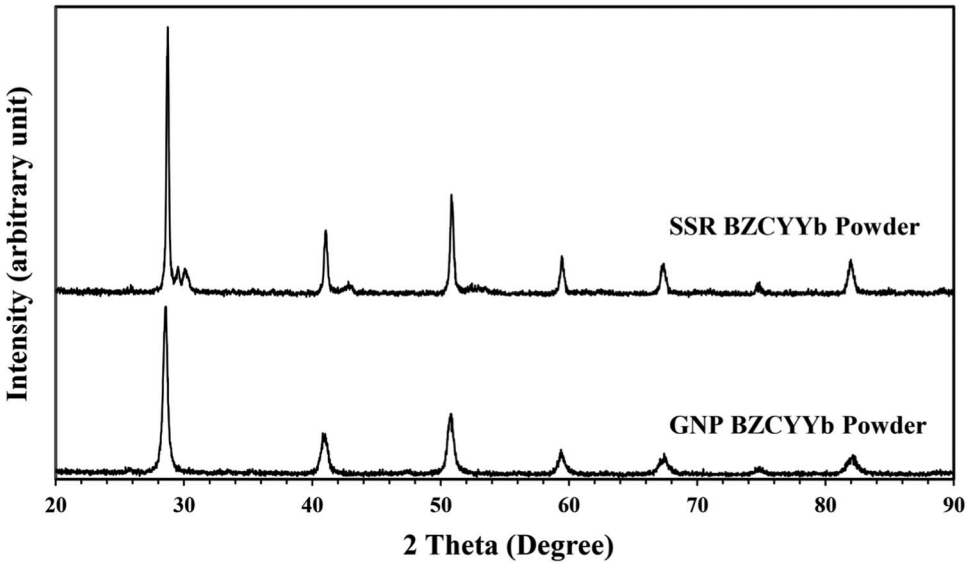

Figure 1. XRD pattern comparison between BZCYYb powders synthesized by GNP followed by calcination at 1100°C for 5 h and SSR methods, respectively.

and non-stoichiometry compositions) were studied under atmospheres contaminated with different concentrations of CO_2 and H_2S, and the results are discussed and correlated with literature.

Experimental

BZCYYb powder with nominal composition of $BaZr_{0.1}Ce_{0.7}Y_{0.1}Yb_{0.1}O_{3-\delta}$ was synthesized by both solid-state reaction (SSR) and glycine nitrate process (GNP) followed by calcination. For SSR, the synthesis process follows that described in the literature.[7] In short, $BaCO_3$ (#14341, Alfa Aesar, 99.8%), ZrO_2 (#11395, Alfa Aesar, 99+%), CeO_2 (#11329, Alfa Aesar, 99.5%), Y_2O_3 (#44286, Alfa Aesar, 99.9%), and Yb_2O_3 (#11191, Alfa Aesar, 99.9%) powders were mixed according to stoichiometry composition and ball-milled in IPA for 24 h followed by drying in oven and calcination at 1100°C for 10 h. The milling-drying-calcination process was repeated once to remove carbonates and obtain pure perovskite phase. Non-stoichiometric BZCYYb powder with nominal composition of $Ba_{0.95}Zr_{0.1}Ce_{0.7}Y_{0.1}Yb_{0.1}O_{3-\delta}$ (i.e., 5 at.% deficiency in Ba) was also synthesized with the similar SSR process. As for the GNP method, stoichiometry amounts of $Ba(NO_3)_2$ (#A11305, Alfa Aesar, 99%), $ZrO(NO_3)_2 \bullet xH_2O$ (#43224, Alfa Aesar, 99.9%), $Ce(NO_3)_3 \bullet 6H_2O$ (#11329, Alfa Aesar, 99.5%), $Y(NO_3)_3 \bullet 6H_2O$ (#12898, Alfa Aesar, 99.9%), and $Yb(NO_3)_3 \bullet xH_2O$ (#12901, Alfa Aesar, 99.9%) powders were dissolved in DI water. Typically, ~30 g of total metal salts were dissolved in 100 g of DI water. Glycine (#G8898, Sigma Aldrich, 99+ %) was then added to the solution with 1:1 glycine to total metal ions molar ratio. Typically 50 ml of solution was heated in a Pyrex glass beaker on a hot plate set at 540°C. After water was completely evaporated, auto-ignition process occurred, and a very fine white powder was produced. The powder was then calcinated in air at different temperatures in the range of 800 to 1100°C for 2–5 h to study the formation of the perovskite phase.

For sintering, the synthesized BZCYYb powders were pressed into disks with diameter of 10 mm at pressure of ~130 MPa. The pressed disks were placed on Al_2O_3, Pt, ZrO_2, CeO_2, and BZCYYb substrates to study the effects of different substrates on sintering of this material. Green disks were sintered in air inside a box furnace (Lindberg Blue M). The disks were sintered in two different configurations: one is called "unprotected" in the following in which the green disk was in direct contact with the substrate (alumina or other substrates); the other is called "protected" in the following in which one green BZCYYb disk was sandwiched between similar BZCYYb green disks and then further covered by loose BZCYYb powders around it to avoid contact with substrates (following the procedure described by Rainwater[19]). Samples were sintered for 5 and 10 h at different temperatures from 1400°C to 1600°C to investigate the effects of time and temperature on sintering. Sample geometric dimensions were measured after sintering to estimate the relative density, and the weight-loss during sintering was also recorded for both samples sintered under "protected" and "unprotected" conditions. To study the effect of sintering aid, 1 wt.% of NiO was added to BZCYYb powder as previously reported,[8] and the green disks were then sintered in air at 1400°C for 5 h under protected condition.

For CO_2 and H_2S stability tests, both BZCYYb powder and sintered disks were exposed to certain gas atmospheres (gas mixture composition all specified by volume) in a tube furnace typically for 24 h at 750°C. For stability against CO_2, BZCYYb was exposed to 100% CO_2, 50% CO_2/50% H_2, and 50% CO_2/50% Ar. As for H_2S stability test, BZCYYb was exposed to gas mixtures of 100 ppm H_2S balanced by H_2 (100 ppm H_2S/H_2) and also to 50 ppm H_2S/50 vol. % H_2/50 vol. % Ar.

X-ray analysis was done by using SIEMENS diffractometer D5000. FE-SEM analysis was performed by JEOL JSM-6330F. To calculate the average grain diameter of the disks after sintering computer programmed image analysis was performed on SEM images. To study in-situ weight loss of BZCYYb powder, DSC analysis was carried out using TA Instruments SDT 600 in platinum crucibles, and powders were heated up from room temperature to 1500°C in air with heating rate of 10°C/min.

Results and Discussion

Synthesis of BZCYYb via GNP process and comparison with SSR method.— Figure 1 shows the XRD patterns of BZCYYb powders synthesized by conventional SSR method and GNP method followed by calcination at 1100°C for 5 h, respectively. The BZCYYb powder produced by GNP method showed fewer amounts of impurities compared with SSR BZCYYb. It is also noted that, unlike using GNP for synthesizing materials such as lanthanum strontium manganese oxide ($La_{1-x}Sr_xMnO_{3-\delta}$), right after GNP combustion, XRD analysis of the product showed a doped ceria pattern and the perovskite structure was not observed.[7] Only after subsequent calcination of the GNP combustion product, pure perovskite BZCYYb phase formed, as shown in Figure 2. Besides, in GNP technique because of the better contact between starting materials and also homogenous distribution of the precursors in the aqueous solution, single-phase perovskite BZCYYb could be obtained at significantly lower temperature for shorter

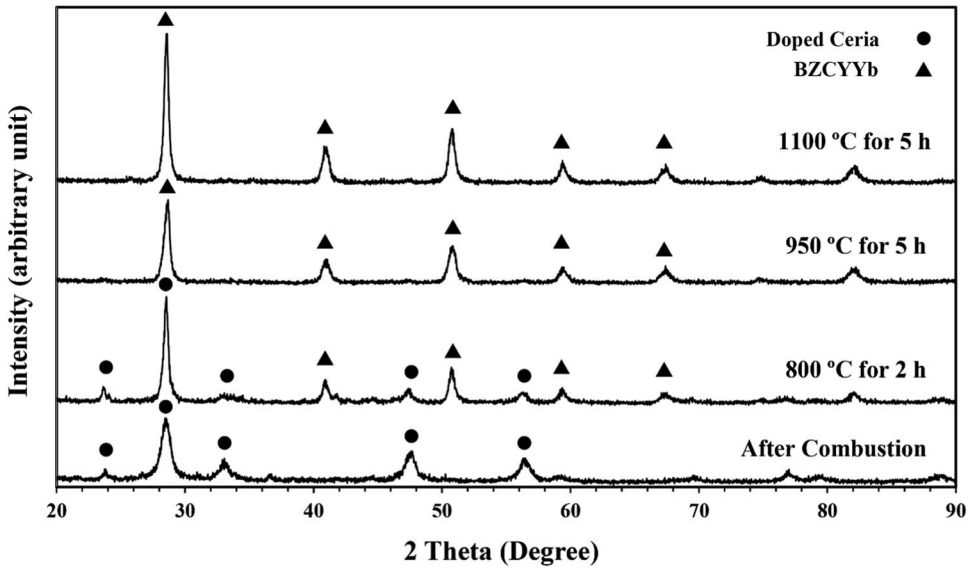

Figure 2. XRD pattern of the BZCYYb powder directly after synthesis and after each calcination step. As it is shown, the as synthesized powder does not show perovskite structure and just after calcination the BZCYYb phase forms.

time compared with SSR method such as 5h of calcination at 950°C. The results are also in agreement with Zhou's work on synthesis of BZCYYb by EDTA assisted GNP technique.[16] Morphology of the GNP-BZCYYb and SSR-BZCYYb powders are shown in Figure 3. As it can be seen, GNP method produces homogenous and finely dispersed powder with particle size of ∼100 nm compared with the typical morphology observed for the SSR powder with larger particles that are strongly bonded together.

Figure 4 shows SEM images of GNP and SSR BZCYYb disks sintered under "protected" condition (i.e., with protective BZCYYb disks and powder layer) in an alumina crucible at 1550°C for 10 h. The samples sintered from GNP powder showed similar density compared to SSR ones but with reduced grain size, which is in agreement with literature[16,20] and expected as powders with finer particle size typically have better sinterability and help maintain a finer structure after sintering.[21,22] In addition, it is noted that GNP powder is easier to compact and gives better visual homogeneity after sintering.

Reaction of BZCYYb with substrates and barium loss during sintering.— In this study it was observed that sintering BZCYYb green disks in direct contact with alumina, zirconia, and cerium oxide substrates at high temperature (e.g., 1550°C) leads to breakdown of the single-phase perovskite structure and formation of doped cerium oxide on the side of the disks in contact with these substrates, which was not reported previously for BZCYYb. Figure 5 shows XRD pattern of the BZCYYb disks sintered on different substrates at 1550°C for 10 h. As seen, the BZCYYb material reacts with alumina and zirconia substrates at that temperature and disintegration of perovskite structure occurs, which is similar to earlier reports on different materials such as $BaCe_{0.8}Y_{0.2}O_3$ (BCY20) and $BaZr_xCe_{0.9-x}Y_{0.1}O_3$ (BZCY).[13,19,23,24] Interestingly, as shown in Figure 5, our results indicate that this material also reacts with cerium oxide substrate at 1550°C and forms mixtures of BZCYYb-doped CeO_2 ceramics. In comparison, sintering this material on platinum substrate covered with platinum cap did *not* lead to noticeable change in BZCYYb XRD pattern and single-phase perovskite structure was maintained even at sintering temperatures

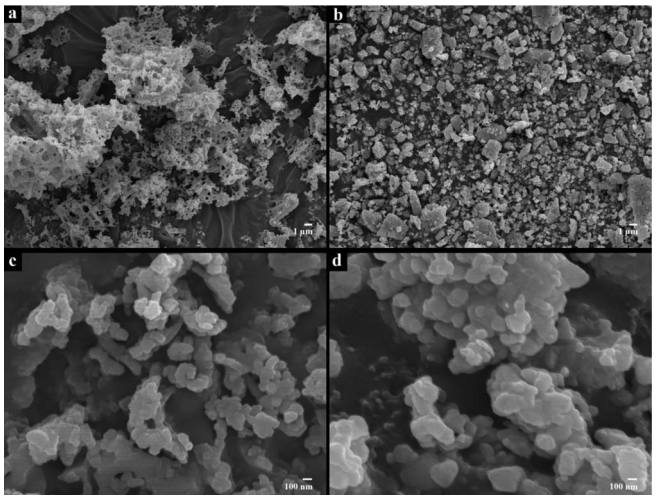

Figure 3. SEM micrographs of (a) and (c): GNP BZCYYb powder, (b) and (d): SSR BZCYYb powders. As typical for GNP method, the GNP BZCYYb showed an ash like structure with finer particle size compared to SSR BZCYYb. In both powders some agglomeration was observed as it is shown in (c) and (d).

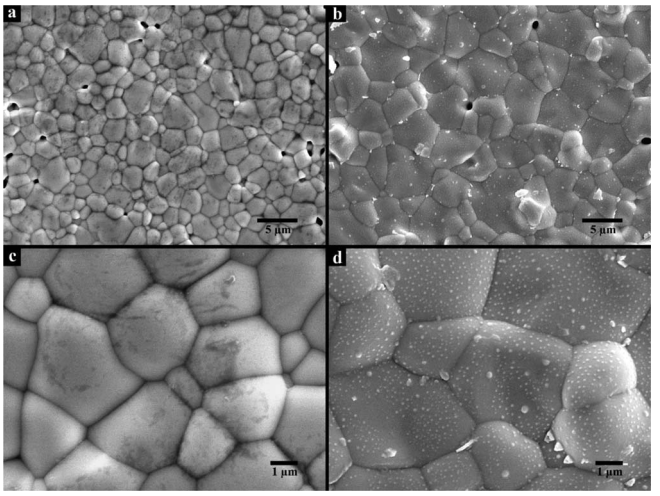

Figure 4. SEM images of (a) GNP BZCYYb and (b) SSR BZCYYb disks sintered at 1550°C for 10 h using a protective BZCYYb layer around the samples. (c) and (d) show higher magnification SEM image of GNP and SSR BZCYYb disks, respectively.

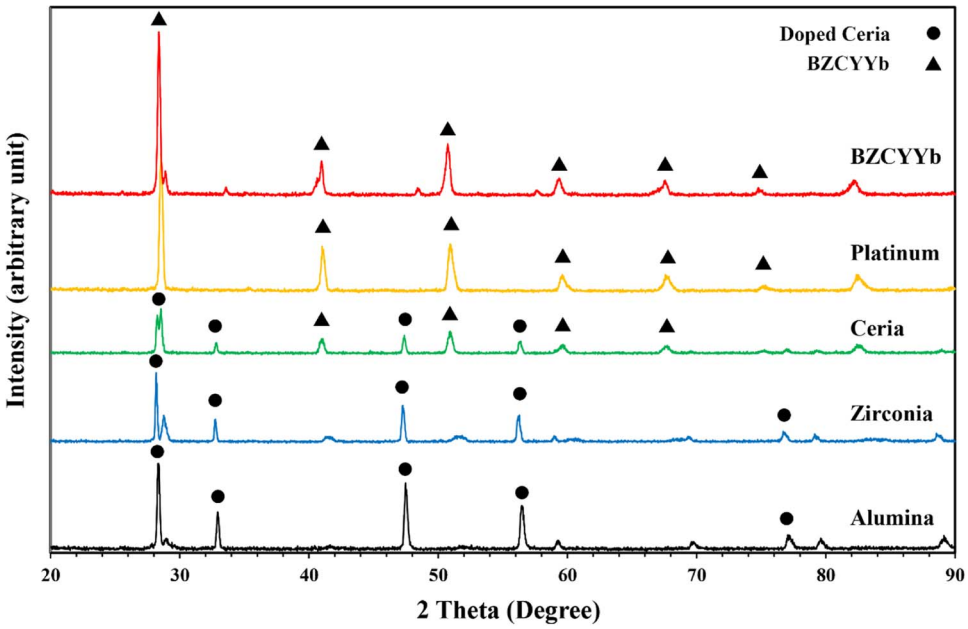

Figure 5. XRD pattern of the BZCYYb disks sintered on alumina, zirconia, ceria, platinum and BZCYYb substrates at 1550°C for 10 h. By using BZCYYb protective layer and platinum substrate and cap, the samples did not show any change in their structure after sintering; however, for those samples sintered directly on alumina and zirconia substrates, the perovskite structure was disintegrated to doped cerium oxide. BZCYYb Sample sintered on ceria substrate was decomposed to BZCYYb + ceria.

as high as 1550°C. In addition, BZCYYb disk and powder can also serve as a protective layer around the green disk to help sinter this material on alumina crucible[19] and no phase change was observed in XRD patterns when green disks were sintered under such "protected" condition.

The greater tendency of BaO to diffuse into alumina and zirconia substrates and react to form even more stable products, is the main reason for the disintegration of BZCYYb material (and doped barium cerate in general) when it is in contact with substrates such as alumina or zirconia at high temperature (e.g., 1550°C in this case). To confirm this, Figure 6 shows XRD pattern of the *alumina substrate* in contact with BZCYYb disk after sintering at 1550°C for 10 h, which clearly shows the formation of $BaAl_2O_4$ phase on the Al_2O_3 substrate. Such observation is consistent with early reports on similar materials such as $BaCe_{0.8}Y_{0.2}O_3$.[14,24] To understand the temperature at which the reaction between BZCYYb and Al_2O_3 starts to occur, DSC analysis of the pure BZCYYb powder and 50 wt.% BZCYYb-50 wt.% Al_2O_3 powder mixture was carried out and the corresponding results are shown in Figure 7. To our surprise, BZCYYb shows really high reactivity with Al_2O_3 when the two materials are intimately mixed with higher contact area than the case for sintering: the BaO-Al_2O_3 reaction peaked at temperature as low as ~ 950°C as evidenced by the endothermic peak for the mixture of these powders when compared to the pure BZCYYb trend in DSC analysis. Figure 8 shows XRD patterns of the 50 wt.% BZCYYb-50 wt.% Al_2O_3 powder mixture right after cold pressing and also after heat-treatment at 1000°C for 2 h, which suggests extensive reaction as evidenced by the complete change of XRD pattern after the heat-treatment.

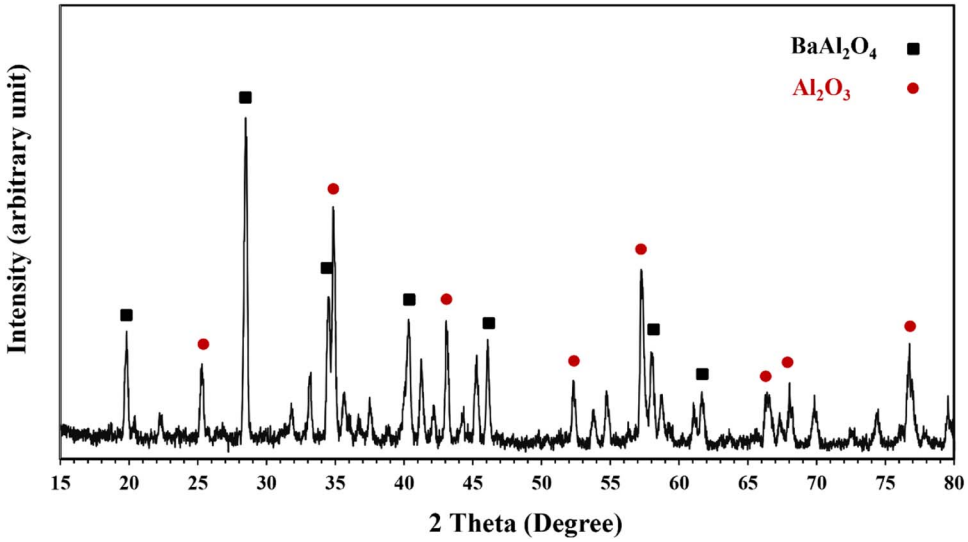

Figure 6. XRD pattern of the alumina crucible directly in contact with BZCYYb disk after sintering at 1550°C for 10 h. Formation of $BaAl_2O_4$ phase confirmed BaO and alumina reaction and the fact that major Ba loss happens through diffusion of Ba to alumina crucible.

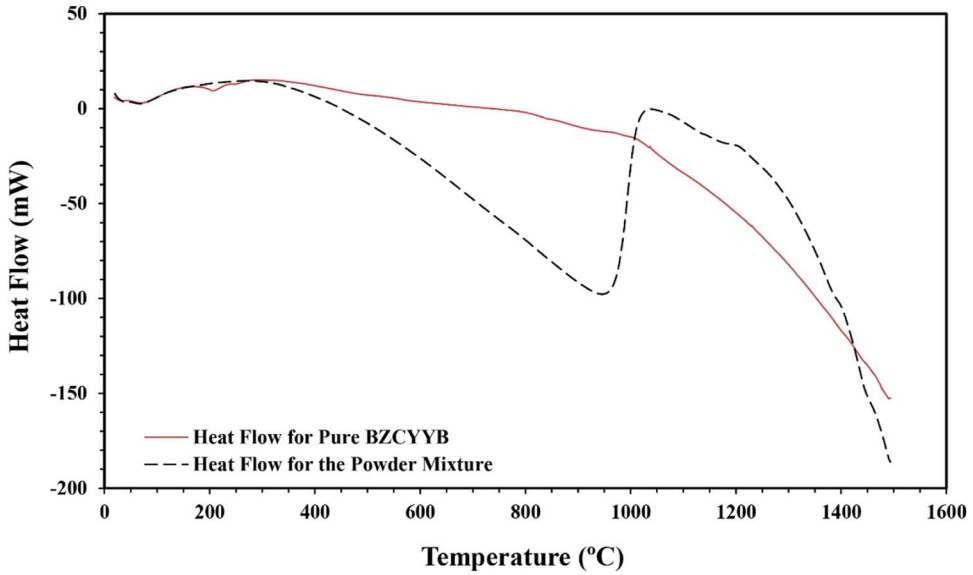

Figure 7. DSC analysis of pure BZCYYb powder and 50 wt.% BZCYYb - 50 wt.% Al_2O_3 mixture heated up to 1500°C with heating rate of 10°C/min on platinum crucibles. The mixture of BZCYYb and Al_2O_3 showed an endothermic peak at ~ 950°C, which confirms the high reactivity of BZCYYb material with alumina.

In the case of BZCYYb reactivity toward CeO_2 substrate, from first glance, it is hard to understand the extent of reaction as the product would still be a type of doped $BaCeO_3$. However, based on the BaO-CeO_2 phase diagram,[25] significant (BaO-CeO_2) liquid solution phase exists at temperatures above ~1480°C (with solubility not yet well established). When the BZCYYb disk is sintered above CeO_2 disk to high temperatures such as 1550°C, re-distribution of BaO in the BZCYYb-CeO_2 system may occur leading to the observed reaction.

Apart from the phase change as identified by XRD analysis, it is also noted that significant weight change may occur during sintering of BZCYYb material.[26] Figure 9 illustrates the measured weight change and corresponding estimated Ba loss (by assuming the sample weight loss come only from BaO loss) of the samples sintered on alumina substrates under "protected" (i.e., with additional protective BZCYYb disks and powder on top and bottom, as explained earlier) and "unprotected" (i.e., BZCYYb disk in direct contact with substrate) conditions. Higher weight loss (and Ba loss) was observed for samples sintered at higher temperatures or for longer time, indicating more Ba diffusion from BZCYYb to alumina crucible in the BaO-Al_2O_3 reaction under this sintering conditions.

In addition, BaO evaporation due to material transport from BZCYYb material surface to furnace wall (which consists primarily of Al_2O_3) through gas-phase transport mechanism is believed to be another reason for weight loss during sintering.[27,28] Our experiments showed that for BZCYYb sintering in Pt crucibles, if a Pt cover was not used, higher weight loss was observed under the same sintering condition. Furthermore, the top surface (i.e., the side facing air) of the BZCYYb disk showed partial disintegration of perovskite phase and formation of doped ceria, while the bottom side kept perovskite

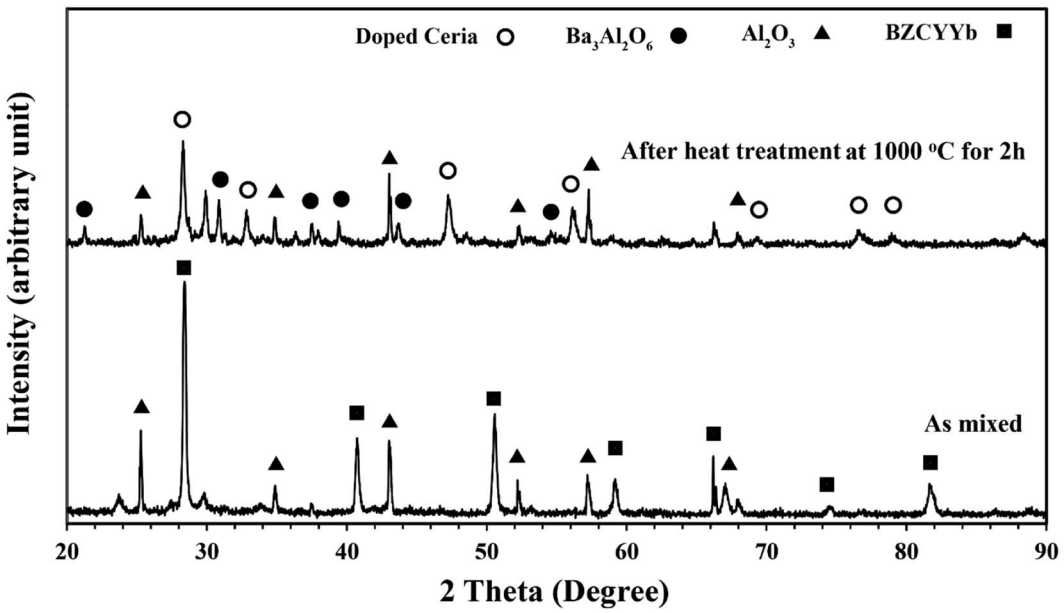

Figure 8. XRD pattern of a disk pressed from 50 wt.% BZCYYb - 50 wt.% Al_2O_3 mixture, before (as-mixed) and after heat-treatment at 1000°C for 2 h.

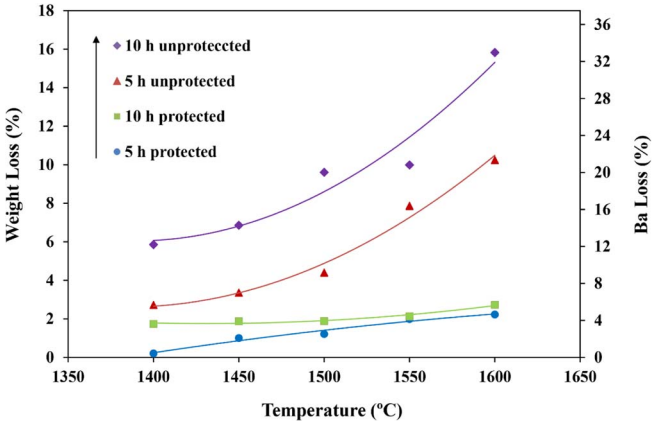

Figure 9. Weight loss (left Y axis) and corresponding Ba loss (right Y axis) of the BZCYYb disks sintered under BZCYYb layer "protected" and "unprotected" conditions for 5 h and 10 h at different temperatures.

structure. This strongly suggests BaO loss also occurs through vapor phase and the use of platinum cap helps to mitigate BaO loss through gas-phase transport.

From the comparison between samples sintered under "protected" versus "unprotected" condition, it is clear that the protective BZCYYb layer can, up to a limit, act as a sacrificing barrier to barium loss in the samples. Correlating the weight loss to XRD data for samples sintered under different conditions, the BZCYYb material can sustain around 5 molar percent of Ba loss without inducing significant structural change (most of the unprotected samples showed phase decomposition after sintering). Higher values of Ba loss result in poorly sintered disks and decomposition of perovskite structure to doped cerium oxide. Increasing Zr content in the composition improves thermal-chemical stability of this material by helping the perovskite structure to withstand higher values of Ba deficiency but often at the expense of reduced ionic conductivity.[1–3,7,13]

Effect of sintering conditions and addition of sintering aid on densification.— As stated before, only sintering on Pt substrate with Pt cover or under "protected" conditions lead to relative pure perovskite BZCYYb sintered disks. As Pt substrate and cover are not very practical for industrial production, the remaining sintering research was done under protected conditions. As expected, increasing time and temperature of sintering, resulted in BZCYYb disks with higher relative density. SEM micrographs of samples sintered at temperatures ranging from 1400°C to 1600°C for 10 h on alumina crucibles under protected conditions are shown in Figure 10a to 10e. Sample porosity decreased as temperature increased up to 1550°C. At 1600°C, observed porosity (lower density) is due to some Ba loss and disintegration of perovskite structure. This was confirmed by XRD analysis and minor peaks for doped ceria was observed in the sample sintered at 1600°C. The SEM image of the sample sintered in Pt crucible with Pt cover at 1550°C for 10 h also showed high density, as shown in Figure 10f. Figure 11 shows relative density of the samples sintered at different temperatures for time periods of 5 and 10 h.

As it was previously reported by Liu et al.[8] adding 1% NiO as sintering aid to the BZCYYb powder can significantly improve sintering of this material. Figure 12 shows comparison of SEM images of a BZCYYb-1% NiO disk with pure BZCYYb sintered at 1400°C for 5 h on alumina crucible under protected condition. Similar to earlier report,[8] adding 1 wt.% NiO significantly promotes grain growth and disks sintered at 1400°C for 5 h showed average grain diameter of 3–4 μm. This is comparable to that of GNP BZCYYB disks sintered for 10 h at higher temperature of 1550°C. The underlying reason for the effect of NiO is probably related to the fact that the BaO-NiO system shows a low melting point of ∼1250°C and below for a broad range of composition (e.g., including $BaNiO_2$).[29] Although BZCYYb does not show high reactivity toward NiO causing formation of other phases, it is hypothesized that there is a BaO-type impurity in the BZCYYb ceramics that might still combine with NiO at elevated temperature, leading to liquid phase sintering, which helps improving the densification process. Similar sintering aid effects were also observed for other oxides such as ZnO that also form liquid at lower temperatures.[30]

Chemical stability in H_2S and CO_2 contaminated atmospheres.— Figure 13 and 14, show XRD patterns of stoichiometric and A-site 5% Ba-deficient BZCYYb powders exposed to different H_2S and CO_2 contaminated atmospheres, respectively. Our results indicate that stoichiometric BZCYYb is stable in atmospheres containing less than 50 ppm H_2S contaminated H_2 at typical fuel cell operating temperature of 750°C. This is in good agreement with the previous report.[7] However, our experiments shown in Figure 13 suggest BZCYYb would react with 100 ppm H_2S and results in formation of barium sulfide after 24 h. Similar results were observed for

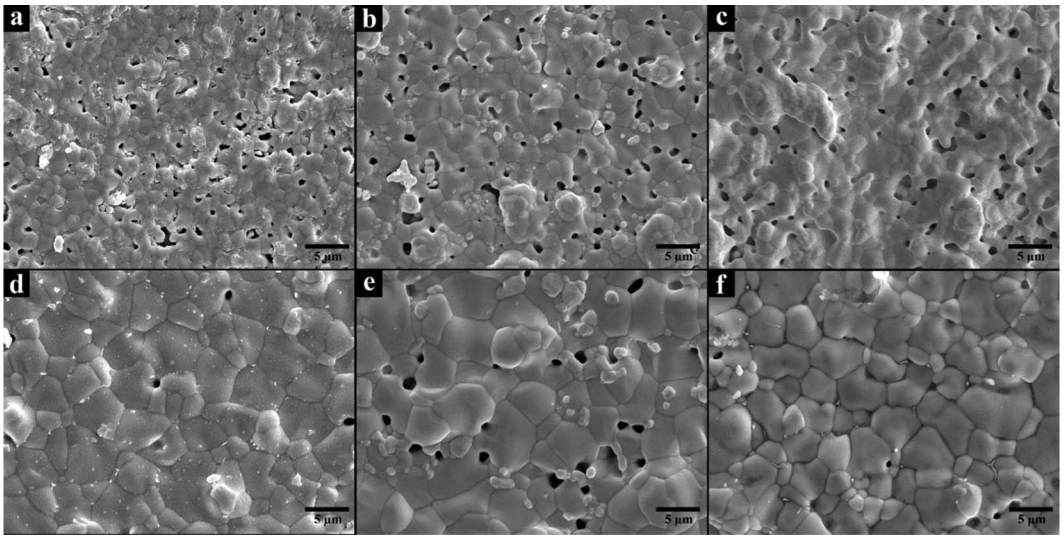

Figure 10. SEM micrographs of BZCYYb disks sintered at (a) 1400°C, (b) 1450°C, (c) 1500°C, (d) 1550°C, and (e) 1600°C for 10 h on alumina crucible under "protected" condition (covered with BZCYYb powder). (f) SEM image of BZCYYb disk sintered on platinum substrate while covered with platinum cap at 1550°C for 10 h.

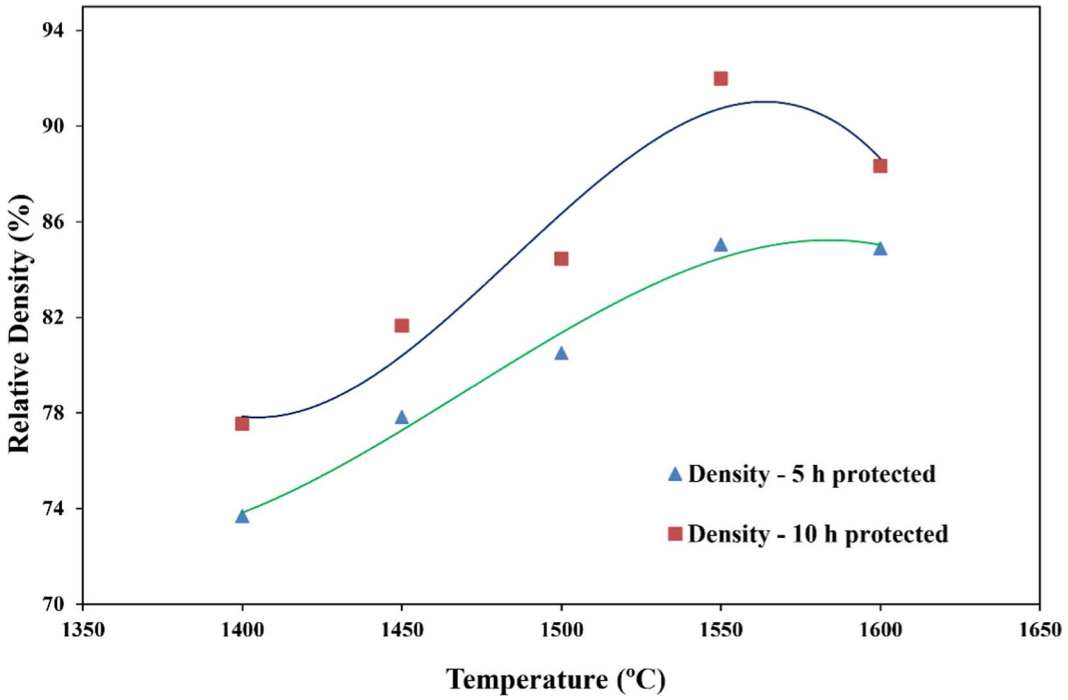

Figure 11. Relative density for BZCYYb disks sintered under protected and unprotected conditions.

BZCYYb disks sintered at 1550°C for 10 h under protected conditions. In addition, as shown in Figure 13, compared with stoichiometric BZCYYb, the A-site 5% Ba deficient BZCYYb (nominal composition of $Ba_{0.95}Zr_{0.1}Ce_{0.7}Y_{0.1}Yb_{0.1}O_{3-\delta}$) appears to have even lower stability and reacts with 50 ppm H_2S to form BaS. This seems counter intuitive as A-site Ba deficiency should in principle have less Ba to react with H_2S. Further investigation is needed to understand such phenomenon.

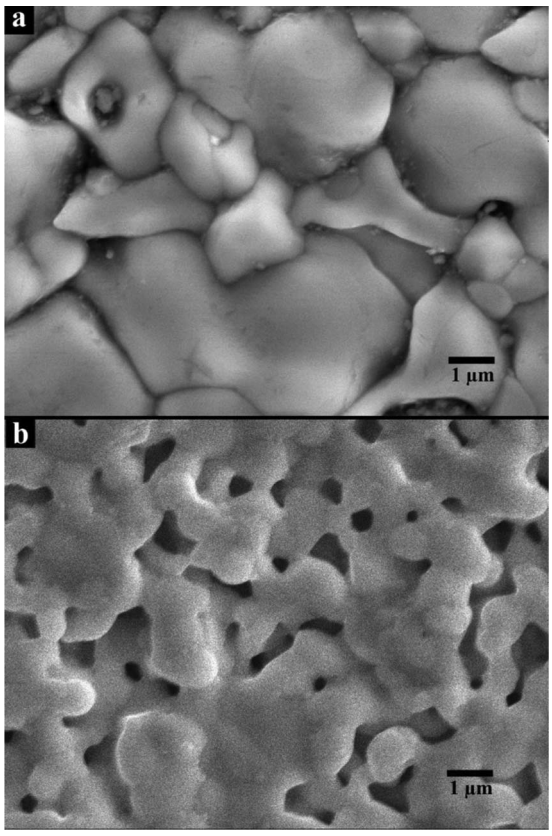

Figure 12. SEM images of (a) the BZCYYb-1% NiO disk sintered at 1400°C for 5 h (b) Pure BZCYYb disk sintered at 1400°C for 5 h. Sintering was done under "protected" conditions for both samples.

In our experiment, BZCYYb showed relatively high reactivity toward CO_2. For example, as shown in Figure 14, our results showed partial decomposition of BZCYYb to barium carbonate and doped ceria in 50% CO_2 balanced by either Ar or H_2 at 750°C after 24 h. BZCYYb disks sintered at 1550°C for 10 h under protected condition showed similar behavior as BZCYYb powder in CO_2 contaminated atmospheres. This is different from the earlier report by Yang et al.[7] reporting no decomposition for this material after 300 h of exposure to fuel mixture of 50% CO_2/50% H_2. The fundamental reason for such discrepancy is not yet known at this moment. Nevertheless, it is noted for the system of doped Ba(Ce, Zr)O_3, partial substitution of Ce with Zr can help increasing chemical stability of doped barium cerate oxides.[1–3,7,13] Though, as explained in various reports[1–3,13] small contents of Zr ($\leq\sim$0.3) in the composition usually does not contribute to significant changes in chemical stability of these family of oxides. For example, Zhong[13] reported that $BaCe_{0.9-x}Zr_xY_{0.1}O_{2.95}$ material containing less than 0.4 moles of Zr in the composition reacts with CO_2 atmosphere at 900°C. It is hypothesized that part of the difference might come from the variation in the A to B-site non-stoichiometry. As shown in Figure 14, no fundamental difference in stability was observed for 5% Ba deficient BZCYYb, which still showed partial decomposition of the perovskite phase and formation of $BaCO_3$.

Conclusions

Yttrium and ytterbium co-doped barium cerate-zirconate oxide electrolyte material, $BaZr_{0.1}Ce_{0.7}Y_{0.1}Yb_{0.1}O_{3-\delta}$ (BZCYYb), was synthesized by both conventional solid state reaction (SSR) and glycine nitrate process (GNP) methods. The GNP method yield doped ceria with amorphous barium oxide species right after combustion, which turned into fine crystalline BZCYYb phase upon subsequent heat-treatment above ~950°C. Apart from reducing the synthesis time and temperature, the GNP method appears superior to SSR method in

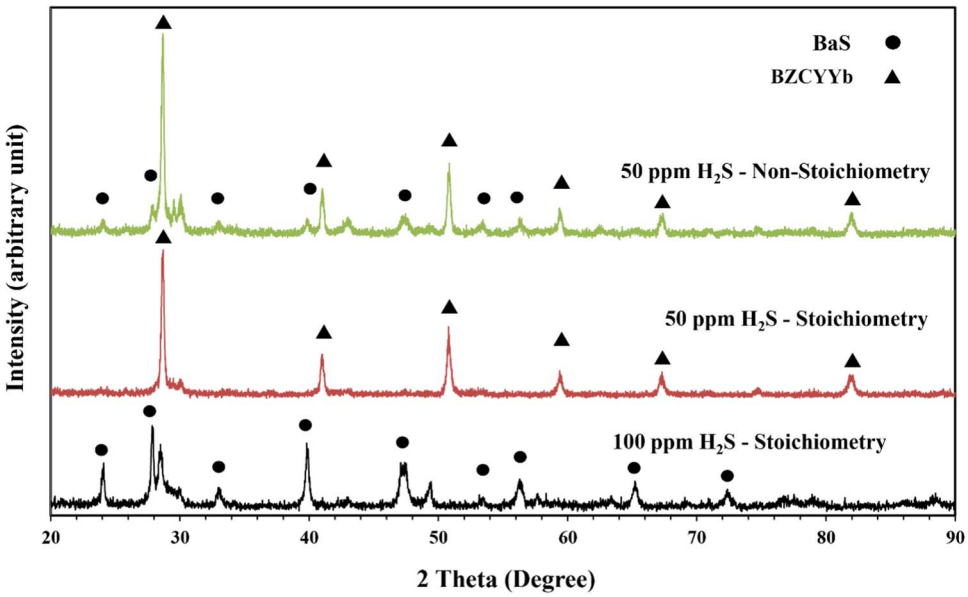

Figure 13. XRD patterns of stoichiometric and non-stoichiometric (5% Ba-deficient) BZCYYb powders after exposure to H_2 atmosphere contaminated with 100 ppm H_2S balanced by H_2 (100 ppm H_2S/H_2) and 50 ppm H_2S/50% H2/50% Ar atmospheres at 750°C for 24 h.

terms of improved product purity and reduced particle size. On the other hand, BZCYYb, despite its high proton conductivity, still shows relatively high reactivity with alumina, zirconia and cerium oxide substrates during sintering and great care should be taken to avoid such reactions, which lead to Ba loss and even disintegration of the perovskite phase. Our results showed sintering BZCYYb on platinum crucible while covering it with a platinum cap or using a protective BZCYYb powder around the sample could significantly reduce Ba loss and maintain the perovskite structure at high temperatures, which is mandatory for sintering BZCYYb to high densities. Experiments also showed BZCYYb has high reactivity toward CO_2 and H_2S down to 100 ppm. A-site barium deficiency in the BZCYYb structure seems to cause further reduction in chemical stability of this material under both CO_2 and H_2S atmospheres.

Acknowledgment

The authors thank Florida International University (FIU) College of Engineering for new faculty start-up funding support. The authors would also like to thank Dr. Alex Franco from FIU for his help in performing thermal analysis on samples. We also acknowledge the support of Advanced Materials Engineering Research Institute (AMERI) at FIU in providing access to different materials preparation and characterization facilities.

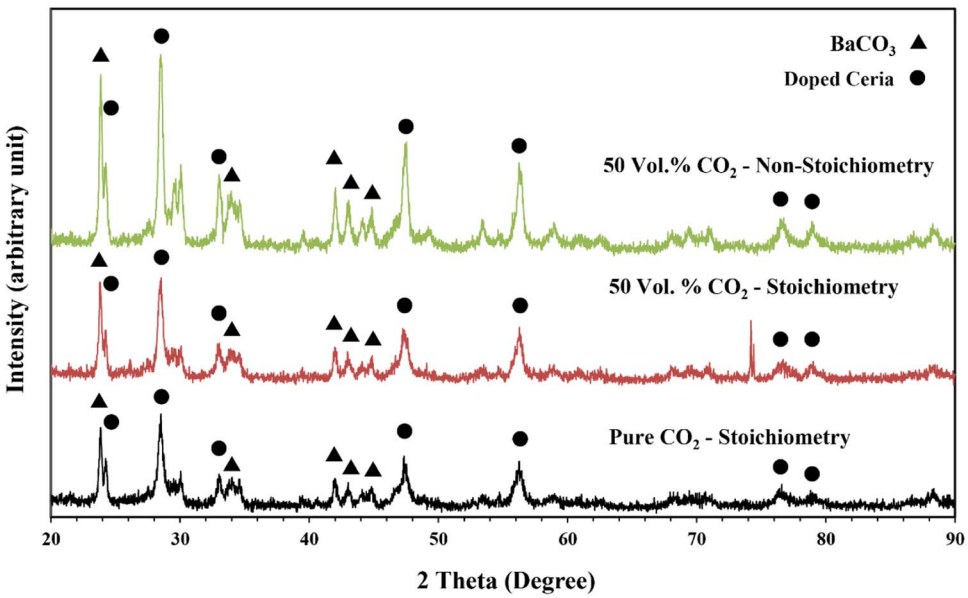

Figure 14. XRD pattern of stoichiometric and non-stoichiometric (5% Ba-deficient) BZCYYb powders after exposure to pure CO_2 and 50 CO_2% Ar/50% H_2 atmospheres at 750°C for 24 h.

References

1. E. Fabbri, D. Pergolesi, and E. Traversa, *Chem. Soc. Rev.*, **39**, 4355 (2010).
2. J. W. Fergus, *J. Power Sources*, **162**, 30 (2006).
3. E. Fabbri, D. Pergolesi, and E. Traversa, *Adv. Mater.*, **24**, 195 (2012).
4. Y. Ling, X. Yao, X. Zhang, X. Liu, and B. Lin, *Int. J. Hydrogen Energ.*, **37**, 5940 (2012).
5. L. Malavasi, C. A. J. Fisher, and M. S. Islam, *Chem. Soc. Rev.*, **39**, 4370 (2010).
6. H. Ding, Y. Xie, and X. Xue, *J. Power Sources*, **196**, 2602 (2011).
7. L. Yang, Sh. Wang, K. Blinn, Mi. Liu, Z. Liu, Z. Cheng, and M. Liu, *Science*, **326**, 126 (2009).
8. Y. Liu, L. Yang, Mi. Liu, Z. Tang, and M. Liu, *J. Power Sources*, **196**, 9980 (2011).
9. H. Ding and X. Xue, *J. Power Sources*, **195**, 7038 (2010).
10. F. Zhao, C. Jin, C. Yang, S. Wang, and F. Chen, *J. Power Sources*, **196**, 688 (2011).
11. R. Muccillo and E. N. S. Muccillo, *ECS Trans.*, **35**(1), 1251 (2011).
12. J Zhang, F. Liang, B. Chi, J. Pu, and L. Jian, *J. Power Sources*, **200**, 29 (2012).
13. Z. Zhong, *Solid State Ionics*, **178**, 213 (2007).
14. A. Subramaniyan, J. Tong, R. P. O'Hayre, and N. M. Sammes, *J. Am. Ceram. Soc.*, **94**(6), 1800 (2011).
15. S. Wang, L. Zhang, L. Zhang, K. Brinkman, and F. Chen, *Electrochim Acta*, **87**, 194 (2013).
16. X. Zhou, L. Liu, J. Zhen, Sh. Zhu, B. Li, K. Sun, and P. Wang, *J. Power Sources*, **196**, 5000 (2011).
17. N. Nguyen and H. Yoon, *J. Power Sources*, **231**, 213 (2013).
18. S. Sengodan, M. Liu, T. Lim, M. Lie, and G. Kim, *J. Electrochem Soc.*, **161**(5), F668 (2014).
19. B. H. Rainwater, *M.Sc. thesis*, Georgia Institute of Technology, August 2012.
20. L. Yang, C. Zuo, and M. Liu, *J. Power Sources*, **195**, 1845 (2010).
21. P. L. Chen and I. W. Chen, *J. Am. Ceram. Soc.*, **80**(3), 637 (1997).
22. C. P. Camron and R. Raj, *J. Am. Ceram. Soc.*, **71**(12), 1031 (1988).
23. F. Chen, O. T. Sørensen, G. Menga, and D. Penga, *J. Mater. Chem.*, **7**(3), 481 (1997).
24. J. Guan, S. E. Dorris, U. Balachandran, and M. Liu, *J. Electrochem. Soc.*, **145**(5), 1780 (1998).
25. J. P. Guha and D. Kolar, *J. Mater. Sci.* **6**, 1174 (1971).
26. A. VahidMohammadi and Z. Cheng, *Proceedings of 39th Int'l Conf. & Expo on Advanced Ceramics & Composites (ICACC)*, 2015.
27. S. J. L. Kang, *Sintering Densification, Grain Growth, and Microstructure*, Elsevier, Oxford, 2005.
28. M. Mazaheri, A. M. Zahedi, and S. K. Sadernezhaad, *J. Am. Ceram. Soc.*, **91**(1), 56 (2008).
29. http://www.crct.polymtl.ca/fact/documentation/TDNucl/BaO-NiO.jpg, Consulted on March 2015.
30. P. Babilo and S. M. Haile, *J. Am. Ceram. Soc.*, **88**(9), 2362 (2005).